stant temperature of 40 °C. Kinetics data were then derived from ^1H NMR spectra as described above. The results of this experiment are tabulated in Table I.

Reaction of 3 or *trans*-3-d_1 with Diphenylacetylene in the Presence of 2-d_2 or 2. 3 (20 mg, 0.073 mmol) was placed in a 5-mm NMR tube along with diphenylacetylene (52 mg, 0.289 mmol). The tube was then attached to a Teflon stopcock with a ground-glass joint, cooled to −50 °C, and degassed. A 500-μL amount of toluene along with 37 μL of 2-d_2 (0.289 mmol) was then vacuum transferred into the tube. After the contents were warmed to room temperature and mixed well, the tube was placed in a constant-temperature bath maintained at 40 °C. After ca. 1 half-life, ^2H NMR spectroscopy indicated that 4% of the total deuterium had been incorporated into the metallacycle. After 7 h, the reaction had proceeded to completion, and 1.7% of the deuterium had been incorporated into 7. Exactly the same procedure was followed for the reaction of *trans*-3-d_1 with diphenylacetylene in the presence of 2. After 7 h, ^2H NMR spectroscopy indicated that the deuterated 3,3-dimethyl-1-butene contained 7.5% of the cis isomer.

Reaction of *trans*-3-d_1 with Diphenylacetylene. trans-3-d_1 (21 mg, 0.076 mmol) was placed into a 5-mm NMR tube attached to a ground-glass joint along with diphenylacetylene (54 mg, 0.3 mmol). A Teflon needle valve adapter was attached and the apparatus evacuated on a vacuum line. Approximately 500 μL of toluene was vacuum transferred into the tube, and the tube was sealed. The tube was heated to 40 °C. After 2 h (ca. 1 half-life), ^2H NMR spectroscopy showed *trans*-2-d_1 (δ 4.84), 7-d_1 (δ 3.38), and *trans*-3-d_1 (δ 2.17). Only a trace of *cis*-3-d_1 and no *cis*-3-d_1 could be detected. After 12 h at 40 °C, the reaction was complete, and the ratio of *trans*-2-d_1 to 7-d_1 was 1.37/1.0.

Reaction of 3-d_2 with Diphenylacetylene. A mixture of 21 mg of 3-d_2 (0.076 mmol) and 54 mg (0.30 mmol) of diphenylacetylene was loaded into a 5-mm NMR tube attached to a ground-glass joint. A Teflon needle valve adapter was attached and the apparatus evacuated on a vacuum line. Approximately 500 μL of toluene was vacuum transferred into the tube, and the tube was sealed. The sample was heated at 40 °C for 12 h. ^2H NMR spectroscopy indicated that the ratio of 2-d_2 to 7-d_2 was 2.2/1.0.

Reaction of 3-d_5 with 8. A mixture of 14 mg of 3-d_5 (0.049 mmol) and 14 mg of 8 (0.048 mmol) was loaded into a 5-mm NMR tube attached to a ground-glass joint. A Teflon stopcock was then attached, and the tube was evacuated on a vacuum line. Approximately 500 μL of benzene-d_6 was vacuum transferred into the tube, and the tube was sealed. The tube was heated to 50 °C. After 1 h, ^1H NMR spectroscopy indicated resonances due to protons incorporating into the α positions of 3, at δ 2.17, 1.86.

Metathesis of *trans*-3-d_1 with 2. This reaction was run with molar ratios of *trans*-3-d_1 to 2 of 2/1 and 10/1. *trans*-3-d_1 (21 mg, 0.076 mmol) was loaded into a 5-mm NMR tube attached to a ground-glass joint. A Teflon stopcock was attached, and the tube was evacuated. A 500-μL of amount of toluene and 2 (20 μL, 0.155 mmol) were vacuum transferred into the tube. The tube was heated at 40 °C for 1 h. $^2H\{^1H\}$ NMR spectroscopy indicated that the ratio of *trans*-2-d_1 (δ 4.84) to *cis*-3-d_1 (δ 1.86) was 3.4/1. The ratio of *trans*-2-d_1 to *cis*-2-d_1 was 18.7/1. When the experiment was repeated with a molar ratio of *trans*-3-d_1 to 2 of 10/1, after 1 h at 40 °C, the ratio of *trans*-2-d_1 to *cis*-3-d_1 was 3.5/1, and the ratio of *trans*-2-d_1 to *cis*-2-d_1 was 14/1.

Metathesis of *trans*-3-d_1 with 3,3-Dimethyl-1-pentene. *trans*-3-d_1 (120 mg, 0.433 mmol) was loaded into a small Schlenk tube. 3,3-Dimethyl-1-pentene (425 mg, 4.33 mmol) and 1.5 mL of toluene were added via syringe. The mixture was then cooled to −196 °C and evacuated. Then it was heated to 40 °C for 65 min. All volatiles were removed in vacuo. The metallacycles were dried at room temperature an additional 1 h under high vacuum. Diphenylacetylene (232 mg, 1.3 mmol) was added to the Schlenk tube along with 1.0 mL of toluene. The mixture was then heated to 40 °C for 12 h. All volatiles were vacuum transferred into another vessel. The volatiles contained 2 (d_0 and d_1) and 3,3-dimethyl-1-pentene (d_0 and d_1) as determined by GC/MS. The 3,3-dimethyl-1-butenes were separated from the 3,3-dimethyl-1-pentenes by preparative GC (Durapak, 120 C, 20 ft). $^2H\{^1H\}$ NMR spectroscopy of 3,3-dimethyl-1-pentene showed two signals of approximately equal intensity at δ 4.89 and 4.92. In the ^2H spectrum two overlapping doublets were observed. The peak entered at δ 4.89 had J(H–D) = 2.56 Hz, and the peak at δ 4.92 had J(H–D) = 1.59 Hz. From the magnitude of the coupling constants, the δ 4.89 and 4.92 peaks are assigned to *cis*-3,3-dimethyl-1-pentene-*1*-d_1 and to *trans*-3,3-dimethyl-1-pentene-*1*-d_1, respectively. Examination of deuterated 2 by ^2H NMR spectroscopy indicated only a trace of *cis*-2-d_1 had been formed during the reaction.

Acknowledgment. We gratefuly acknowledge the support of the National Science Foundation (Grant CHE 8016528) and the Department of Energy and the use of the Southern California Regional NMR Facility (NSF Grant 7916324A1).

Registry No. 1, 67719-69-1; 1-d_2, 83664-91-9; 2, 558-37-2; 2-d_3, 83664-87-3; 3, 75687-68-2; 3-*d*, 83664-92-0; 3-d_2, 83664-93-1; 3-d_5, 83664-94-2; 4, 79389-13-2; 5, 81602-83-7; 7, 74834-09-6; 8, 83664-95-3; $AlMe_3$, 75-24-1; Cp_2TiCl_2, 1271-19-8; $Cp_2\overline{TiClAlMeClCH_2}$, 77933-59-6; 3,3-dimethyl-1-butene, 558-37-2; 2-d_1, 57002-05-8; 2-d_2, 83664-88-4; 3,3-dimethyl-1-pentene, 3404-73-7; 2,3-dimethyl-1-butene, 563-78-0; α-methylstyrene, 98-83-9; (*Z*)-α-methylstyrene-d_1, 21370-59-2; 3,3-dimethyl-1-pentene, 3404-73-7; *cis*-3,3-dimethyl-1-pentene-*1*-d_1, 83664-89-5; *trans*-3,3-dimethyl-1-pentene-*1*-d_1, 83664-90-8.

Preparation, Properties, and Kinetics of the Reaction with Tributyltin Hydride of Manganese(0) Radicals $Mn(CO)_3(R_3P)_2$[1a]

Sharon B. McCullen[1b] and Theodore L. Brown*

Contribution from the School of Chemical Sciences, University of Illinois, Urbana, Illinois 61801. *Received April 23, 1982*

Abstract: Persistent manganese(0) radicals, $Mn(CO)_3L_2$·, where L = P(*n*-Bu)$_3$, P(*i*-Bu)$_3$, P(*i*-Pr)$_3$, or P(O-*i*-Pr)$_3$, have been prepared by a photochemical route. The radicals exhibit absorptions in the 600–1200-nm range, ascribed to transitions involving largely metal-centered orbitals. Reaction with CCl_4 gives rise to the corresponding $Mn(CO)_3L_2Cl$, predominantly the 2,4-L_2-1-Cl isomer. The most likely geometry of the radicals is a distorted square pyramid, with phosphorus ligands in trans-basal positions. Reaction of $Mn(CO)_3L_2$· with $HSuBu_3$ gives rise to mainly $Mn(CO)_3L_2H$, with small amounts of $Mn(CO)_3L_2SnR_3$. The reaction is first order each in $Mn(CO)_3L_2$· and $HSnR_3$ and appears to proceed via a simple H atom transfer. The bimolecular rate constants at 20 °C in hexane are 10.7, 0.786, 0.110, and 2.0 × 10^{-3} M^{-1} s^{-1} for L = P(*n*-Bu)$_3$, P(*i*-Bu)$_3$, P(O-*i*-Pr)$_3$, and P(*i*-Pr)$_3$, respectively.

There has been a lively interest during the past few years in the properties of metal carbonyl radicals.[2] For the most part, such radicals, which are most conveniently formed by metal–metal bond homolysis, atom transfer, or electron transfer, are not

0002-7863/82/1504-7496$01.25/0

persistent. That is, the average lifetime of the radical in solution is relatively short mainly because of metal–metal bond formation. Nevertheless, it has been possible to deduce many properties of the radicals from spectroscopic and kinetics studies. Thus it has been learned that radicals are exceptionally labile with respect to substitution processes, e.g., replacement of CO by a phosphine,[3-7] and that they readily undergo atom transfer[8] or electron transfer[9] reactions under appropriate conditions.

There are few reports in the literature of stable, persistent zerovalent metal carbonyl radicals. Substituted metal carbonyl radical species may form an equilibrium mixture containing both the paramagnetic mononuclear and the spin-paired dinuclear forms. Examples include $(\eta^5\text{-}C_5H_5)Cr(CO)_3\cdot$,[10] $(\eta^3\text{-}C_3H_5)Fe(CO)_2PH_3\cdot$,[11] and $[P(OC_2H_5)_3]_2Mn(CO)_3\cdot$.[12] Earlier reports of persistent substituted metal carbonyl radicals have been shown to be incorrect.[13] The predominant species in these cases was apparently the hydride, formed by hydrogen atom transfer from some component present in the system.

Zerovalent manganese radicals $Mn(CO)_3L_2\cdot$ (L = phosphine), prepared via photochemical substitution, have been reported.[12] The equilibria involved are those shown in eq 1–4. The equi-

$$Mn_2(CO)_8L_2 \xrightleftharpoons{h\nu} 2Mn(CO)_4L\cdot \quad (1)$$

$$Mn(CO)_4L\cdot + L \rightleftharpoons Mn(CO)_3L_2 + CO \quad (2)$$

$$Mn(CO)_3L_2\cdot + Mn(CO)_4L\cdot \rightleftharpoons Mn_2(CO)_7L_3 \quad (3)$$

$$2Mn(CO)_3L_2\cdot \rightleftharpoons Mn_2(CO)_6L_4 \quad (4)$$

librium in (2) is shifted to the right by periodic removal of CO during irradiation. When L is sufficiently large, the equilibrium in eq 4 lies far to the left.

We report here the preparation and characterization of several new $Mn(CO)_3L_2\cdot$ radicals via photochemical substitution. In the absence of O_2 or other radical scavengers, the radicals so formed are stable in hydrocarbon solution for several weeks. It is thus possible to carry out studies of their chemical and physical properties. We have studied the products and kinetics of the reactions with tributyltin hydride, $HSnBu_3$. Among the questions of interest are the dependence of the reaction rate on the size and electronic characteristics of L, and the pathway by which reaction proceeds. The most obvious a priori mechanistic possibilities are a direct atom transfer or loss of L or CO followed by an oxidative addition of the H–Sn bond.

Experimental Section

Materials. $Mn_2(CO)_{10}$ was purchased from Pressure Chemical Co., and sublimed at 50 °C (0.1 mmHg) before use. Tri-*n*-butylphosphine ($P(n\text{-}Bu)_3$), triisobutylphosphine ($P(i\text{-}Bu)_3$), and triisopropyl phosphite ($P(O\text{-}i\text{-}Pr)_3$) obtained from Strem Chemical Co. were distilled from CaH_2 under reduced pressure of N_2. Triisopropylphosphine ($P(i\text{-}Pr)_3$), Strem Chemical Co., was distilled from CaH_2 under atmospheric pressure of N_2. Hexane was passed through 6–12 mesh silica gel, followed by distillation from sodium benzophenone ketyl. $HSn(n\text{-}Bu)_3$ was obtained from Alfa Chemicals and used without further purification. $[Mn(CO)_4P(n\text{-}Bu)_3]_2$, $[Mn(CO)_4P(i\text{-}Bu)_3]_2$, $[Mn(CO)_4P(O\text{-}i\text{-}Pr)_3]_2$, and $[Mn(CO)_4P(i\text{-}Pr)_3]_2$ were synthesized according to literature procedures.[5,14]

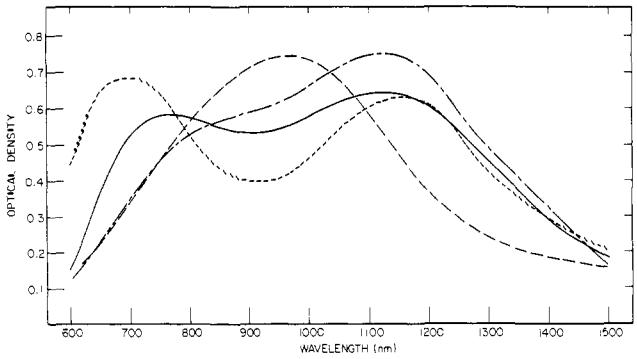

Figure 1. Electronic spectra of $Mn(CO)_3L_2\cdot$ in hexane: (—) $Mn(CO)_3[P(n\text{-}Bu)_3]_2\cdot$; (— -) $Mn(CO)_3[P(i\text{-}Bu)_3]_2\cdot$; (– –) $Mn(CO)_3[P(O\text{-}i\text{-}Pr)_3]_2\cdot$; (- - -) $Mn(CO)_3[P(i\text{-}Pr)_3]_2\cdot$.

Table I. IR Absorption Bands Assigned to $Mn(CO)_3L_2\cdot$ in Hexane

L	ν_{CO}, cm^{-1}	
$P(n\text{-}Bu)_3$	1860 (sh)	1855 (s)
$P(i\text{-}Bu)_3$	1860 (sh)	1855 (s)
$P(O\text{-}i\text{-}Pr)_3$	1893 (s)	1875 (s)
$P(i\text{-}Pr)_3$	1863 (sh)	1857 (s)

Photolysis Experiments. The photochemical substitution reaction of $Mn_2(CO)_8L_2$ (5×10^{-3} M) with L (1×10^{-2} M) in hexane were carried out in a quartz reaction vessel attached to a vacuum line for degassing and removal of CO during reaction. The solution was irradiated with a General Electric 275-W sunlamp. Repeated freezing and pump-off of CO permits substantial conversion to the monomeric, disubstituted radical. However, the practical extent of conversion varies with L. Only for $P(i\text{-}Bu)_3$ was a nearly quantitative conversion possible over a period of several hours irradiation. Traces of CO remaining in solution are apparently effective in replacing L in $Mn(CO)_3L_2\cdot$. Attempts to isolate the highly reactive radicals have thus far been unsuccessful. The UV–visible or EPR spectra of the irradiated solutions were recorded without opening the reaction chamber, by transferring a portion of the solution to an attached side arm containing the appropriate cell. Samples for IR analysis were obtained by removal of a sample from the reaction chamber in an inert atmosphere box.

Reaction of $Mn(CO)_3L_2\cdot$ with $HSnBu_3$. In a typical experiment the $Mn(CO)_3L_2\cdot$ solutions were prepared as described above, in suitable concentrations such that the absorbance of the IR band in the 1855–1875-cm^{-1} region due to the radical was 0.30–0.35 in a 1.0-mm path length IR cell. The solution was transferred to a brown amber bottle and sealed with a rubber septum. Similarly, several $HSnBu_3$ solutions of variable, known concentration were prepared in sealed amber bottles. All solution preparations were performed in an inert atmosphere box. The stopped-flow apparatus and data acquisition system utilized in these experiments have been described elsewhere.[9a,15] The rate of disappearance of $Mn(CO)_3L_2\cdot$ following mixing of the reactant solutions was determined by monitoring the IR absorbance at 1855 cm^{-1} for L = $P(n\text{-}Bu)_3$, $P(i\text{-}Bu)_3$, or $P(i\text{-}Pr)_3$, or at 1875 cm^{-1} for L = $P(O\text{-}i\text{-}Pr)_3$.

Instrumentation. All IR spectra were obtained with a Beckman IR-4240 spectrophotometer. The IR instrument was fitted with a germanium filter to remove UV or visible light from the IR source beam. Electronic spectra were recorded on solutions in matched 0.2-cm quartz cells with a Cary Model 14 spectrophotometer. FT ^{1}H NMR spectra were obtained on a 360-MHz instrument in the NSF regional NMR

(1) (a) This research was supported by the National Science Foundation via research Grants CHE-79-13-8010730 and CHE-81-19525. (b) Sohio Fellow, 1980–1981.

(2) Brown, T. L. *Ann. N.Y. Acad. Sci.* **1980**, *333*, 80.
(3) Wrighton, M. S.; Ginley, D. S. *J. Am. Chem. Soc.* **1975**, *97*, 2065.
(4) (a) Fawcett, J. P.; Jackson, R. A.; Poë, A. J. *J. Chem. Soc., Chem. Commun.* **1975**, 733. (b) DeWit, D. G.; Fawcett, J. P.; Poë, A. J. *J. Chem. Soc., Dalton, Trans.* **1976**, 528.
(5) Kidd, D. R.; Brown, T. L. *J. Am. Chem. Soc.* **1978**, *100*, 4095.
(6) Byers, B. H.; Brown, T. L. *J. Am. Chem. Soc.* **1977**, *99*, 2527.
(7) Fox, A.; Malito, J.; Poë, A. *J. Chem. Soc., Chem. Commun.* **1981**, 1052.
(8) Ginley, D. S.; Wrighton, M. S. *J. Am. Chem. Soc.* **1975**, *97*, 3533.
(9) (a) Absi-Halabi, M.; Brown, T. L. *J. Am. Chem. Soc.* **1977**, *99*, 2982. (b) Forbus, N. P.; Oteiza, R.; Smith, S. G.; Brown, T. L. *J. Organomet. Chem.* **1980**, *193*, C71–C74.
(10) (a) Adams, R. D.; Collins, D. E.; Cotton, F. A. *J. Am. Chem. Soc.* **1974**, *96*, 749. (b) Madach, T.; Vahrenkamp, H. *Z. Naturforsch. B: Anorg. Chem., Org. Chem.* **1978**, *33B*, 1301.
(11) (a) Murdock, H. D.; Lucken, E. A. C. *Helv. Chim. Acta* **1964**, *47*, 1517. (b) Muetterties, E. L.; Sosinsky, B. A.; Zamaraev, K. I. *J. Am. Chem. Soc.* **1975**, *97*, 5299.
(12) Kidd, D. R.; Cheng, C. P.; Brown, T. L. *J. Am. Chem. Soc.* **1978**, *100*, 4103.
(13) (a) Miller, J. R.; Myers, D. H. *Inorg. Chim. Acta* **1971**, *5*, 215. (b) Cox, D. J.; Davis, R. *J. Organomet. Chem.* **1980**, *186*, 339.
(14) (a) Lewis, J.; Nyholm, R. S.; Osborne, A. G.; Sandhu, S. S.; Stiddard, M. H. B. *Chem. Ind. (London)* **1963**, 1398. (b) Osborne, A. G.; Stiddrd, M. H. B. *J. Chem. Soc.* **1964**, 634.
(15) (a) Bellus, P. Ph.D. Thesis, University of Illinois, Urbana-Champaign, 1980. (b) Blumer, D. J. Ph.D. Thesis, University of Illinois, Urbana-Champaign, 1981.

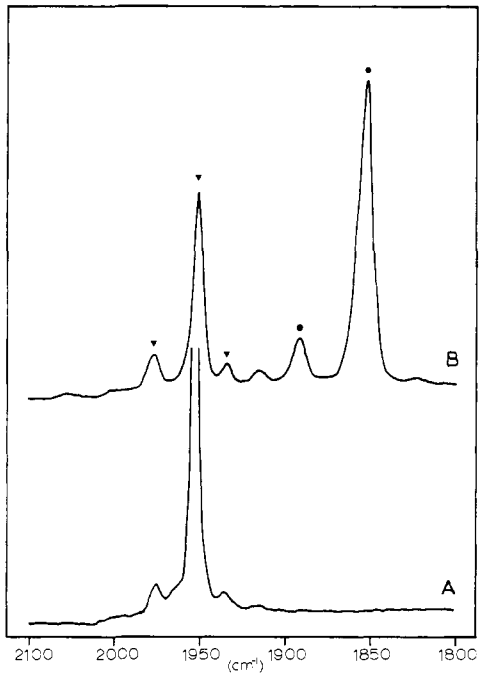

Figure 2. IR spectra following the photolysis of $Mn_2(CO)_8[P(i\text{-}Bu)_3]_2$ with $P(i\text{-}Bu)_3$ in hexane: (A) initial; (B) after several hours photolysis. The absorptions are assigned as follows: (▼) to $Mn_2(CO)_8[P(i\text{-}Bu)_3]_2$; (■) to $HMn(CO)_3[P(i\text{-}Bu)_3]_2$; (●) to $Mn(CO)_3[P(i\text{-}Bu)_3]_2$·.

facility at the University of Illinois.

Results

Preparation and Characterization of $Mn(CO)_3L_2$·. When a degassed hexane solution of $Mn_2(CO)_8L_2$ with L is irradiated for several hours with periodic removal of CO, the solution changes color from red-orange to green. The green color results from absorption of radiation of wavelengths less than 500 nm due to unreacted $Mn_2(CO)_8L_2$ and to broad absorption in the region 600–1500 nm, $\epsilon_{max} \sim 500\ M^{-1}\ cm^{-1}$, as shown in Figure 1. The electronic spectrum of $Mn(CO)_5$·, generated by pulse radiolysis of $Mn_2(CO)_{10}$ or $Mn(CO)_5Br$, exhibits a broad absorption with λ_{max} at 830 nm (ϵ 800 $M^{-1}\ cm^{-1}$).[16] By analogy with this observation we propose that $Mn(CO)_3L_2$· is responsible for the absorptions in the range 600–1500 nm.

The green solution exhibits an EPR signal. The frozen solution spectra of the radicals are similar to that for $Mn(CO)_3[P(n\text{-}Bu)_3]_2$·, reported earlier. Detailed simulations of the EPR spectra for $Mn(CO)_3L_2$· (L = $P(i\text{-}Bu)_3$, $P(i\text{-}Pr)_3$, and $P(O\text{-}i\text{-}Pr)_3$) will be presented elsewhere.[17] In general, the spectra are consistent with an approximate square-pyramidal geometry about Mn, with hyperfine interaction to both ^{55}Mn ($I = {}^5/_2$) and two equivalent phosphine ligands.

After several hours irradiation of $Mn_2(CO)_8L_2$ with L in hexane, new IR absorption bands appear, as shown in Figure 2. The major reaction product is $Mn(CO)_3L_2$·, with small amounts of $HMn(CO)_3L_2$.[18]

The IR bands in the CO stretching region assigned to $Mn(CO)_3L_2$· are listed in Table I. When the green solution resulting from irradiation is exposed to the atmosphere the IR absorption bands between 1890 and 1850 cm^{-1} disappear. No new carbonyl stretching absorptions are noted.

Addition of CCl_4 to the green solution containing $Mn(CO)_3L_2$· (L = $P(n\text{-}Bu)_3$) leads to new absorption bands at 2025 (w), 2005 (w), 1940 (s), and 1895 (m) cm^{-1}, assigned to 2,4-L_2-1-Cl-$Mn(CO)_3$ and a lesser amount of 2,3-L_2-1-Cl-$Mn(CO)_3$ on the basis of comparison with literature values.[19] Similar observations are made for reaction of CCl_4 with $Mn(CO)_3L_2$· when L is $P(i\text{-}Bu)_3$ or $P(O\text{-}i\text{-}Pr)_3$. The sole product of reaction of $Mn(CO)_3[P(i\text{-}Pr)_3]_2$· with CCl_4 is 2,4-L_2-1-Cl-$Mn(CO)_3$. These products are probably the result of simple chlorine atom transfer from CCl_4 to $Mn(CO)_3L_2$·[8,20] (eq 5).

$$CCl_4 + Mn(CO)_3L_2\cdot \rightarrow CCl_3\cdot + ClMn(CO)_3L_2 \qquad (5)$$

The formation of $HMn(CO)_3L_2$ during photolysis is likely a result of hydrogen atom transfer from a solvent impurity. The amount of $HMn(CO)_3L_2$ formed, deduced by comparative IR intensities of $Mn(CO)_3L_2$· and $HMn(CO)_3L_2$, appears to vary with L; larger concentrations of $HMn(CO)_3L_2$ were formed for the less bulky phosphorus donor ligands.

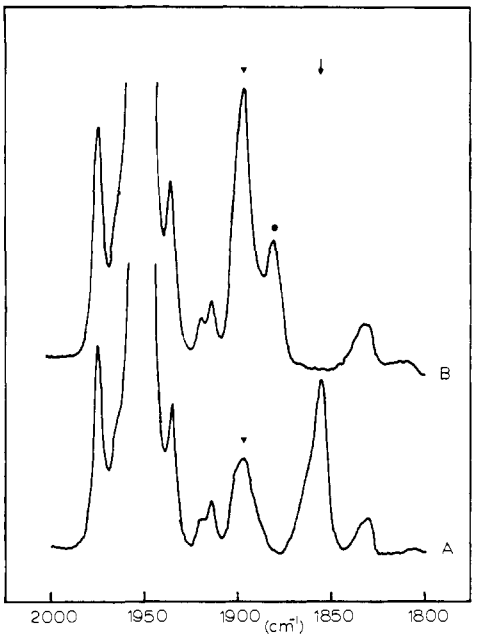

Figure 3. IR spectra following the reaction of $Mn(CO)_3[P(n\text{-}Bu)_3]_2$· with $HSnBu_3$: (A) initial; (B) after reaction. The absorption assigned to $HMn(CO)_3[P(n\text{-}Bu)_3]_2$ is denoted by (▼). The absorption assigned to $Bu_3SnMn(CO)_3[P(n\text{-}Bu)_3]_2$ is denoted by (●). The absorption assigned to $Mn(CO)_3[P(n\text{-}Bu)_3]_2$· is denoted by (↓).

Reaction of $Mn(CO)_3L_2$· with $HSnBu_3$. The reaction of $Mn(CO)_3[P(n\text{-}Bu)_3]_2$· with $HSnBu_3$ results in formation of $HMn(CO)_3[(n\text{-}Bu)_3]_2$. FT ^1H NMR of the reaction product in C_6D_6 solvent reveals a triplet at τ 18.4 due to the product hydride. Lesser amounts of $Bu_3SnMn(CO)_3[P(n\text{-}Bu)_3]_2$ are also formed in the reaction, as shown in Figure 3. Although there are no reports in the literature of $Bu_3SnMn(CO)_3L_2$ compounds, comparison of the IR spectra of $HMn(CO)_5$ and $Ph_3SnMn(CO)_5$ indicates that the corresponding absorption bands lie at lower frequency for the triphenyltin compound.[21,22] Assignment of the absorption at 1875 cm^{-1} to $Bu_3SnMn(CO)_3[P(n\text{-}Bu)_3]_2$ is consistent with this observation.

The disappearance of $Mn(CO)_3[P(n\text{-}Bu)_3]_2$· in hexane at 20 °C follows a pseudo-first-order rate law. A plot of log k_{obsd} vs. log $[HSnBu_3]$ has a slope of 1.0, indicating that the reaction is first-order also in $HSnBu_3$ concentration.

The first-order rate constants for the reaction of $Mn(CO)_3[P(n\text{-}Bu)_3]_2$· with $HSnBu_3$ were observed as a function of temperature in the range 273–295 K. The activation energy, 26.1 kJ mol^{-1}, and the Arrhenius preexponential factor, $3.5 \times 10^3\ s^{-1}$, were determined from a plot of log k_{obsd} vs. $1/T$ (K^{-1}). The enthalpy and entropy of activation are $\Delta H^* = 23.7 \pm 1.3$ kJ mol^{-1}

(16) Waltz, W. L.; Hackelberg, L. M.; Dorfman, L. M.; Wojcicki, A. J. *J. Am. Chem. Soc.* **1978**, *100*, 7259.
(17) Rattinger, G.; Belford, L.; McCullen, S. B.; Walker, H. W.; Brown, T. L., manuscript in preparation.
(18) Ugo, R.; Bonati, F. *J. Organomet. Chem.* **1967**, *8*, 189.
(19) Angelici, R. J.; Basolo, F.; Poë, A. J. *J. Am. Chem. Soc.* **1963**, *85*, 2215.
(20) Abrahamson, H. B.; Wrighton, M. S. *J. Am. Chem. Soc.* **1977**, *99*, 5510.
(21) Braterman, P. S.; Harrill, R. W.; Kaesz, H. D. *J. Am. Chem. Soc.* **1967**, *89*, 2851.
(22) Jetz, W.; Simons, P. B.; Thompson, J. A. J.; Graham, W. A. G. *Inorg. Chem.* **1966**, *5*, 2217.

Table II. Second-Order Rate Constants for Reaction of $Mn(CO)_3L_2\cdot$ with $HSnBu_3$ (1.0×10^{-2} M) at 20 °C in Hexane

L	k, M^{-1} s^{-1}	θ,[a] deg	ν, cm^{-1} [b]
$P(n\text{-}Bu)_3$	10.7	132	2060.3
$P(i\text{-}Bu)_3$	0.786	145	2059.7
$P(O\text{-}i\text{-}Pr)_3$	0.110	130	2075.9
$P(i\text{-}Pr)_3$	2.00×10^{-3}	160	2059.2

[a] Reference 23. [b] A_1 symmetry CO stretching mode of $Ni(CO)_3L$; see ref 23.

and $\Delta S^{\ddagger} = -147 \pm 5$ J K^{-1}, respectively. The reaction of $Mn(CO)_3L_2\cdot$ when L = $P(O\text{-}i\text{-}Pr)_3$, $P(i\text{-}Bu)_3$, or $P(i\text{-}Pr)_3$ with $HSnBu_3$ also results in formation of $HMn(CO)_3L_2$. Except when L is $P(i\text{-}Pr)_3$ small amounts of $Bu_3SnMn(CO)_3L_2$ were also formed. In all cases the rate of reactant disappearance is first order in $[Mn(CO)_3L_2\cdot]$. Except for L = $P(i\text{-}Bu)_3$ the order in $HSnBu_3$ was not tested. However, on the basis of relative rates and product distribution it can be presumed that all reactions are second order overall. Listed in Table II are the calculated second-order rate constants.

Discussion

The photochemical substitution reaction of $Mn_2(CO)_8L_2$ with L results in formation of $Mn(CO)_3L_2\cdot$, which persists in solution as a stable radical when the size of L precludes formation of the metal–metal bond. The electronic spectra of the $Mn(CO)_3L_2\cdot$ radicals are characterized by broad absorption in the 600–1500-nm range, with two absorption maxima for L = $P(n\text{-}Bu)_3$, $P(i\text{-}Bu)_3$, or $P(i\text{-}Pr)_3$, and a single maximum for L = $P(O\text{-}i\text{-}Pr)_3$.

The geometry for $Mn(CO)_5\cdot$ predicted from simple molecular orbital considerations[24,25] and observed in matrix isolation studies[26] is square pyramidal. Similarly, the geometry of the isoelectronic $CO(CN)_5^{3-}$ ion is observed in the solid state to be square pyramidal.[27] This ion exhibits an absorption maximum at 966 nm, ϵ_{max} 233 M^{-1} cm^{-1}.[28]

The expected structure for the $Mn(CO)_3L_2\cdot$ radicals is that of a perturbed square pyramid, with the two phosphine ligands occupying cis or trans basal positions. If the two geometrical forms were of comparable energy, the equilibrium between them would be expected to be quite facile. It is therefore not possible to rigorously deduce the geometry of the radical from the geometry of $Mn(CO)_3L_2Cl$, the product of reaction with CCl_4. The product is likely to be determined by kinetic considerations, i.e., which isomer reacts more rapidly with CCl_4. We might expect that the relative stabilities of the cis and trans isomers will depend mainly on the properties of the phosphines and not be so sensitive to the nature of the axial "ligand". Thus, the fact that the product is predominantly the isomer with trans phosphine ligands suggests that the trans isomer is likely to be the more stable in the radical as well. (Incidentally, conversion of 2,3-$[PR_3]$-1-Br-$Mn(CO)_3$ to the lower energy 2,4-$[PR_3]$-1-Br-$Mn(CO)_3$ form is slow in relation to the time required for formation and analysis for products in the current study;[19] thus, it is unlikely that the product has undergone significant isomerization during the experiment.)

Elian and Hoffmann have given the one-electron energy level diagram for a $Mn(CO)_5\cdot$ species of C_{4v} symmetry, Figure 4.[24] The degeneracy of the d_{xz} and d_{yz} orbitals is removed by the presence of the two phosphines in the basal position, as shown schematically in the figure. If the electronic transitions observed in the visible and near-IR are d–d-like in character, involving promotion of an electron from the d_{xz}, d_{yz} set to the mainly d_{z^2} orbital that contains the unpaired electron, there should be a splitting when the degeneracy of the d_{xz}, d_{yz} orbitals is lifted by the substitution. Because the phosphine ligands are not capable of substantial π bonding with the metal center and because they are strongly σ donor in character, it is reasonable to expect that the d orbitals will be raised in energy in the order $d_{xz} > d_{yz} \sim d_{z^2}$.

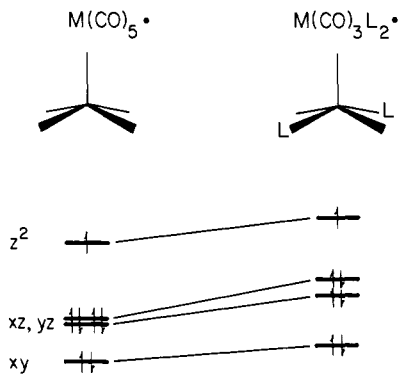

Figure 4. Energy levels of metal-centered orbitals in $M(CO)_5\cdot$ and $M(CO)_3L_2\cdot$.

The observations are in reasonable accord with these expectations. The phosphine-substituted radicals exhibit substantial splitting, and one of the transitions is shifted to longer wavelength relative to the single transition observed for $Mn(CO)_5\cdot$ ($\lambda_{max} \sim$ 830 nm). A single broad transition is observed for the phosphite-substituted radical, as might be expected from the closer similarity of $P(O\text{-}i\text{-}Pr)_3$ to CO in terms of π acceptor character. It is noteworthy, however, that there has nevertheless been a shift to longer wavelength. The simple MO calculations for $M(CO)_5\cdot$ show that the d orbital energy differences are strongly dependent on the angle between the axial and basal M–CO vectors.[24] Portions of the changes in transition energies in $M(CO)_3L_2\cdot$ as compared with $M(CO)_5\cdot$ are thus likely to be due to geometrical changes resulting from the size of the ligands.

A comparison of the behavior of the $Mn(CO)_3[P(n\text{-}Bu)_3]_2\cdot$ and $Mn(CO)_3[P(O\text{-}i\text{-}Pr)_3]_2\cdot$ radicals suggests that both electronic and steric factors are involved in determining the strength of metal–metal bond formation or other aspects of reactivity of the radical. There is no evidence in the visible or IR spectra of metal–metal bond formation in solutions of $Mn(CO)_3[P(n\text{-}Bu)_3]_2\cdot$ as temperature is lowered. By contrast, a green solution of $Mn(CO)_3[P(O\text{-}i\text{-}Pr)_3]_2\cdot$ turns red-orange upon cooling to 0 °C. At the same time the IR absorptions at 1893 and 1875 cm^{-1} due to the radical decrease in intensity while bands at 1957 and 1947 cm^{-1} increase in intensity. These observations suggest that an equilibrium exists, as in eq 6. An equilibrium of this kind was

$$Mn_2(CO)_6[P(O\text{-}i\text{-}Pr)_3]_4 \rightleftarrows 2Mn(CO)_3[P(O\text{-}i\text{-}Pr)_3]_2\cdot \quad (6)$$

proposed earlier for $Mn_2(CO)_6[P(OC_2H_3)_3]_4$.[12] Inasmuch as $P(n\text{-}Bu)_3$ and $P(O\text{-}i\text{-}Pr)_3$ are of comparable size, as measured by their cone angles (Table II), the differences in behavior of the two radicals must be ascribed to the greater π acceptor character of the phosphite.[29]

The reactions of $Mn(CO)_3L_2\cdot$ with $HSnBu_3$ exhibit first-order dependence upon the concentrations of $Mn(CO)_3L_2\cdot$ and $HSnBu_3$. The kinetic observations and the products of the reaction are best accounted for in terms of reactions 7–9. It is interesting that

$$Mn(CO)_3L_2\cdot + HSnBu_3 \underset{k_{-1}}{\overset{k_1}{\rightleftharpoons}} HMn(CO)_3L_2 + \cdot SnBu_3 \quad (7)$$

$$Mn(CO)_3L_2\cdot + \cdot SnBu_3 \xrightarrow{k_2} Bu_3SnMn(CO)_3L_2 \quad (8)$$

$$2Bu_3Sn\cdot \xrightarrow{k_3} Sn_2Bu_6 \quad (9)$$

no $Bu_3SnMn(CO)_3[P(i\text{-}Pr)_3]_2$ was observed as a reaction product when L = $P(i\text{-}Pr)_3$. The bimolecular rate constant for formation of $Mn_2(CO)_8L_2$ from $Mn(CO)_4L\cdot$ radicals has been shown to decrease by more than 2 orders of magnitude when L = $P(i\text{-}Pr)_3$ as compared with L = $P(n\text{-}Bu)_3$.[30] Similarly, the rate constant

(23) Tolman, C. A. *Chem. Rev.* **1977**, *77*, 313.
(24) Elian, M.; Hoffmann, R. *Inorg. Chem.* **1975**, *14*, 1058.
(25) (a) Burdett, J. K. *J. Chem. Soc., Faraday Trans.* **1974**, *70*, 1599. (b) Burdett, J. K. *Inorg. Chem.* **1975**, *14*, 375.
(26) Church, S. P.; Poliakoff, M.; Timney, J. A.; Turner, J. J. *J. Am. Chem. Soc.* **1981**, *103*, 7515.
(27) Brown, L. D.; Raymond, K. N. *Inorg. Chem.* **1975**, *14*, 2590.
(28) Alexander, J. J.; Gray, H. B. *J. Am. Chem. Soc.* **1967**, *89*, 3356.
(29) Jackson, R. A.; Poë, A. *Inorg. Chem.* **1978**, *17*, 997.
(30) Olsen, R. W.; Brown, T. L., manuscript in preparation.

k_2 is likely to be smaller when L is larger. Formation of $R_3SnMn(CO)_3L_2$ is thus inhibited relative to formation of Sn_2R_6 (eq 9).

The differential equations describing the rate processes in eq 7–9 were numerically integrated for various assumed values of the rate constants and initial concentrations of reactants to test the feasibility of the mechanism and to determine the effect of the reverse reaction in eq 7 on the observed kinetics of the reaction of $Mn(CO)_3[P(n\text{-}Bu)_3]_2\cdot$ with $HSnBu_3$. The numerical integration was carried out with a modified version of the program HAVCHM.[31] The requirements were that the observed first-order rate constants, reaction order in $Mn(CO)_3[P(n\text{-}Bu)_3]_2\cdot$ and $HSnBu_3$ and the final product distribution should reproduce the observed values.

The value for k_3 is known:[32] 3.0×10^7 M^{-1} s^{-1}. Values for the other rate constants given in the reaction scheme, eq 7–9, which give the closest match of experimental and calculated results are $k_1 = 9.0$ M^{-1} s^{-1}; $k_{-1} = 1.0 \times 10^3$ M^{-1} s^{-1}; $k_2 = 3.0 \times 10^5$ M^{-1} s^{-1}. The uncertainty in the rate constants is about 20%. The value for k_2, substantially less than the diffusion-controlled rate constant, reflects the expected steric barrier to formation of the Sn–Mn bond. Values for k_{-1} larger than 1.0×10^3 M^{-1} s^{-1} cause the reaction to deviate from first-order kinetics for the disappearance of $Mn(CO)_3[P(n\text{-}Bu)_3]_2\cdot$. The value chosen for k_{-1} is reasonable for a slightly exothermic hydrogen atom transfer reaction. That the model successfully reproduces the first-order dependence upon concentrations of $Mn(CO)_3L_2\cdot$ and $HSnBu_3$, and the closeness of k_1 to the experimental second-order rate constant, supports the mechanism shown in eq 7–9.

The H–Mn bond dissociation energy of $HMn(CO)_5$ is estimated to be 213 kJ mol^{-1} or perhaps a little larger,[33] as compared with 293 kJ mol^{-1} for the H–Sn bond dissociation energy of $HSnBu_3$.[34] The enthalpy of activation for reation of $Mn(CO)_3[P(n\text{-}Bu)_3]_2\cdot$ with $HSnBu_3$ indicates that the H–Sn bond energy can be at most only about 26 kJ mol^{-1} larger than the Mn–H bond energy in $HMn(CO)_3[P(n\text{-}Bu)_3]_2$. This observation is consistent with the suggestion that replacement of CO by a phosphorus donor ligand in a metal carbonyl hydride may result in a higher M–H bond dissociation energy.[6]

The reactions of $Mn(CO)_3L_2\cdot$ with $HSnBu_3$ are affected by both the electronic and steric properties of the phosphorus donor ligands. In the reaction of $HSnBu_3$ and $Mn(CO)_3L_2\cdot$ where L is $P(n\text{-}Bu)_3$ or $P(i\text{-}Pr)_3$ the H–Mn bond energy of the resulting $HMn(CO)_3L_2$ compounds should be nearly the same due to the closely similar electronic properties of the phosphorus donor ligands. Inasmuch as the same bond is broken for the series of reactions, the overall enthalpy change for the reactions involving the three different manganese radicals should be similar. We observe, however, a substantial variation in reaction rates because of variation in the sizes of the ligands. When the phosphorus donor ligand hinders close approach of the hydrogen atom source to the orbital containing the unpaired electron on manganese, the rate of hydrogen atom transfer decreases.

Steric factors in the reactions of $Mn(CO)_3L_2\cdot$ where L is $P(n\text{-}Bu)_3$ or $P(O\text{-}i\text{-}Pr)_3$ with $HSnBu_3$ are roughly constant. The difference in rates for the two reactions is most likely related to a lower H–Mn bond energy in $HMn(CO)_3[P(O\text{-}i\text{-}Pr)_3]_2$.

The reactions of $HSnBu_3$ with several other metal carbonyl radicals, e.g., $Co(CO)_3L\cdot$ or $(\eta^5\text{-}C_5H_5)Mo(CO)_3\cdot$, have been accounted for in terms of an oxidative addition of the H–Sn bond to a 15-electron intermediate, e.g., $Co(CO)_2L$ or $(\eta^5\text{-}C_5H_5)Mo(CO)_2$, formed by loss of CO from the radical.[35,36] The fact that the alternative atom transfer is observed in the reaction of the $Mn(CO)_3L_2\cdot$ radicals can be ascribed to the much lower lability of these phosphorus donor-substituted radicals toward ligand or CO dissociation. We have shown elsewhere that replacement of L or CO by CO in $Mn(CO)_3L_2\cdot$ occurs via an associative rather than dissociative pathway.[37] The rate constants for even these associative pathways are not rapid relative to the observed rate constants listed in Table II for the corresponding radical.

Registry No. $Mn(CO)_3[P(n\text{-}Bu)_3]_2\cdot$, 67551-64-8; $Mn(CO)_3[P(i\text{-}Bu)_3]_2\cdot$, 81971-50-8; $Mn(CO)_3[P(O\text{-}i\text{-}Pr)_3]_2\cdot$, 83634-19-9; $Mn(CO)_3[P(i\text{-}Pr)_3]_2\cdot$, 83634-20-2; $HSnBu_3$, 688-73-3; $[Mn(CO)_4P(i\text{-}Bu)_3]_2$, 83634-21-3; $HMn(CO)_3[P(i\text{-}Bu)_3]_2$, 83649-37-0; $HMn(CO)_3[P(n\text{-}Bu)_3]_2$, 83634-22-4; $Bu_3SnMn(CO)_3[P(n\text{-}Bu)_3]_2$, 83634-23-5; $[Mn(CO)_4P(n\text{-}Bu)_3]_2$, 15609-33-3; $[Mn(CO)_4P(O\text{-}i\text{-}Pr)_3]_2$, 75862-69-0; $[Mn(CO)_4P(i\text{-}Pr)_3]_2$, 75847-41-5; 2,4-$L_2$-1-Cl-$Mn(CO)_3$ (L = $P(n\text{-}Bu)_3$), 63511-10-4; 2,3-L_2-1-Cl-$Mn(CO)_3$ (L = $P(n\text{-}Bu)_3$), 83679-79-2; 2,4-L_2-1-Cl-$Mn(CO)_3$ (L = $P(i\text{-}Pr)_3$], 83634-24-6.

(31) Stabler, R. N.; Chesick, J. P. *Int. J. Chem. Kinet.* **1978**, *10*, 461.
(32) Carlsson, D. J.; Ingold, K. U. *J. Am. Chem. Soc.* **1968**, *90*, 7047.
(33) (a) Connor, J. A. *Top. Curr. Chem.* **1977**, *71*, 71. (b) Connor, J. A.; Zafarani-Moattar, M. T.; Bickerton, J.; El Saied, N. I.; Suradi, S.; Carson, R.; Al Takhin, G.; Skinner, H. A. *Organometallics* **1982**, *1*, 1166.
(34) Jackson, R. A. *J. Organomet. Chem.* **1979**, *166*, 17.
(35) Wegman, R. W.; Brown, T. L. *J. Am. Chem. Soc.* **1980**, *102*, 2494.
(36) Wegman, R. W.; Brown, T. L. *Organometallics* **1982**, *1*, 47.
(37) McCullen, S. B.; Walker, H. W.; Brown, T. L. *J. Am. Chem. Soc.* **1982**, *104*, 4007.